

99mTc-HMPAO SPECT imaging reveals brain hypoperfusion during status epilepticus

Pablo Bascuñana

Medical School Hannover <https://orcid.org/0000-0003-2186-8899>

Bettina J. Wolf

Medizinische Hochschule Hannover

Ina Jahreis

Medizinische Hochschule Hannover

Mirjam Brackhan

Oslo Universitetssykehus

Luis García-García

Universidad Complutense de Madrid Facultad de Farmacia

Tobias L. Ross

Medizinische Hochschule Hannover

Frank M. Bengel

Medizinische Hochschule Hannover

Marion Bankstahl

Tierärztliche Hochschule Hannover

Jens P. Bankstahl (✉ bankstahl.jens@mh-hannover.de)

Medizinische Hochschule Hannover <https://orcid.org/0000-0003-4735-4490>

Short communication

Keywords: brain perfusion, pilocarpine, neuroimaging, epilepsy

Posted Date: September 1st, 2020

DOI: <https://doi.org/10.21203/rs.3.rs-63466/v1>

License:  This work is licensed under a Creative Commons Attribution 4.0 International License.

[Read Full License](#)

Version of Record: A version of this preprint was published at Metabolic Brain Disease on September 27th, 2021. See the published version at <https://doi.org/10.1007/s11011-021-00843-z>.

Abstract

Status epilepticus (SE) is a clinical emergency with high mortality. SE can trigger neuronal death or injury and alteration of neuronal networks resulting in long-term cognitive decline or epilepsy. Among the multiple factors contributing to this damage, imbalance between oxygen and glucose requirements and brain perfusion during SE has been proposed. Herein, we aimed to quantify by neuroimaging the spatiotemporal course of brain perfusion during and after lithium-pilocarpine-induced SE in rats.

To this purpose, animals underwent ^{99m}Tc -HMPAO SPECT imaging at different time points during and after SE using a small animal SPECT/CT system. ^{99m}Tc -HMPAO regional uptake was normalized to the injected dose. In addition, voxel-based statistical parametric mapping was performed.

SPECT imaging showed an increase of cortical perfusion before clinical seizure activity onset followed by regional hypo-perfusion starting with the first convulsive seizure and during SE. Twenty-four hours after SE, brain ^{99m}Tc -HMPAO uptake was widely decreased. Finally, chronic epileptic animals showed regionally decreased perfusion affecting hippocampus and cortical sub-regions.

Despite elevated energy and oxygen requirements, brain hypo-perfusion is present during SE. Our results suggest that insufficient compensation of required blood flow might contribute to the neuronal damage and neuroinflammation, and ultimately to chronic epilepsy generated by SE.

Introduction

Status epilepticus (SE) is a clinical emergency with high morbidity and mortality [1]. It is characterized by continuous epileptic seizure activity and is often of sufficient duration to produce irreversible neuronal damage. SE results from mechanisms leading to seizing activity in combination with failure of the endogenous mechanisms responsible for seizure prevention or termination [1]. Depending on the type and duration of seizures, SE can not only trigger neuronal injury, but also alterations of neuronal networks that may result in long-term cognitive decline or epilepsy [2].

Animal models of SE are currently used to study epileptogenesis and are widely applied to evaluate new anti-seizure and antiepileptogenic treatments [3]. Thus, knowledge of the neuropathology of SE is extensive, but mostly focused on its later consequences. Among animal models, the rat lithium-pilocarpine model is one of the most widely used. After pilocarpine-induced SE, rats show BBB impairment, neuroinflammation, neuronal loss, reactive gliosis (affecting both microglia and astroglia), axonal sprouting and neurotransmitter imbalance among other alterations, finally leading to the development of chronic epilepsy [4–6].

It has been theorized that the damage induced by SE is caused not only by the excessive neuronal activation directly leading to excitotoxicity, but may also be due to an imbalance between oxygen and glucose requirements and sufficient brain perfusion during SE [7]. Perfusion-weighted magnetic resonance imaging (MRI) may be used to investigate perfusion changes during SE in patients or animal

models [7], but needs to be performed under general anesthesia during data acquisition to immobilize the subject. As anesthesia is known to influence brain perfusion [8], this most probably influences study outcome.

SPECT perfusion imaging using ^{99m}Tc -hexa-methyl-propylene-amine-oxime (HMPAO) might be an alternative for investigation of brain perfusion during SE. HMPAO crosses the blood-brain barrier and is converted rapidly from the lipophilic to the hydrophilic state. Thus, it becomes intracellularly trapped. Once trapped in the brain, HMPAO remains stable with little wash-in or wash-out effect [9]. Due to its fast kinetics, ictal ^{99m}Tc -HMPAO SPECT has been widely used for epileptic focus localization in drug-refractory patients [10]. It allows assessment of the brain perfusion state without anesthesia, as the tracer gets trapped in the first minutes after injection [11] and brain retention is very stable. Thus, ^{99m}Tc -HMPAO is clinically injected during acute seizures and scans are performed after the seizure. Similarly, we used ^{99m}Tc -HMPAO SPECT imaging to study brain perfusion before, during and after SE in the widely used lithium-pilocarpine rat model.

Experimental Procedures

Animals

Adult female Sprague-Dawley rats (n = 44; Envigo, Italy) were housed in pairs in individually ventilated bio-containment units under a 14/10-h light/dark cycle with free access to standard laboratory chow and autoclaved tap water. Animals were allowed to adapt to housing conditions and repetitive handling for at least one week before starting the experiments. All the experiments were conducted in accordance with European Communities Council Directive 2010/63/EU and were formally approved by the responsible local authority. Data is reported in accordance with the ARRIVE guidelines.

Status epilepticus induction

SE was induced as described previously [6]. Shortly, rats (n = 36) were pre-treated with lithium chloride (127 mg/kg, p.o.) 14–16 h before pilocarpine injection. Methyl-scopolamine (1 mg/kg, i.p.; Sigma-Aldrich, Germany) was administered 30 min before a bolus injection of pilocarpine hydrochloride (30 mg/kg, i.p.; Sigma-Aldrich, Germany), followed by a maximum of 3 injections of 10 mg/kg at 30 min intervals as needed until SE onset, defined by self-sustained convulsive seizing evaluated as described before [6]. Onset and self-sustainment of SE was defined by continuous visual inspection. Overall, an average pilocarpine dose of 34.40 ± 5.83 mg/kg was needed to induce SE (46 ± 17 minutes until SE induction), without significant differences between groups. SE was interrupted after 90 minutes by repeated administration of diazepam (maximal 25 mg/kg, i.p.; Ratiopharm). To avoid potential influence on tracer distribution, no electrodes were implanted. Therefore, epilepsy stage was confirmed by reporting behavioral seizures happening during daily handling in the animal room. Rats classified as chronic epileptic were those that exhibited at least two generalized spontaneous seizures before SPECT imaging.

SPECT imaging

Awake animals were injected intravenously at different time points with 85.7 ± 12.1 MBq ^{99m}Tc -HMPAO synthesized using a standard preparation kit (Ceretek, GE Healthcare): (i) baseline (naïve animals; $n = 8$), (ii) 15 min after the first pilocarpine injection ($n = 6$), (iii) within seconds after start of the first generalized seizure ($n = 8$), (iv) 15 min after SE onset ($n = 5$), (v) 24 h after SE ($n = 9$), and (vi) in the chronic epileptic stage (12 weeks after SE; $n = 5$). To avoid interference from acute seizures with brain perfusion in the 24 h group, animals were observed for 2 hours before injection, but no such seizures were observed. Animals were anesthetized using isoflurane (1 to 2% in 100% oxygen) 110 minutes after radiotracer injection, placed prone in an imaging chamber (Minerve, France) being continuously warmed, and monitored for heart and respiration rate, maintaining respiratory rate at 60–80 breaths/min for comparable anesthesia depth. The SPECT scan was started 120 minutes after tracer injection with the brain at the center of the field of view using the cadmium zinc telluride detector equipped Explore speCZT camera with a rat 5-pinhole collimator (Trifoil Imaging). Projection data were acquired in step-and-shoot mode with 108 views per pinhole (0.67° increment angle, and 30 s per step) followed by a low-dose computed tomography (CT) scan. Energy threshold was set at 60 keV, with a reconstruction window of 125–150 keV for ^{99m}Tc . Images were reconstructed using maximum likelihood expectation maximization with 50 iterations to a $156 \times 156 \times 216$ image matrix (0.5 mm pixel size).

Image analysis

CT images were fused to an MRI template [12] using PMOD 3.7 software (PMOD Technologies, Switzerland). Subsequently, SPECT images were matched to the template using the corresponding spatial transformation. A region of interest (ROI) atlas [13] was then applied to the co-registered images as previously described [6]. Average total counts for each ROI were calculated and divided by the injected dose. Normalization to a reference region was not performed, as no robust reference region could be identified. Co-registered images were further analyzed by statistical parametric mapping (SPM). Differences in ^{99m}Tc -HMPAO uptake between each time point of interest and baseline were analyzed by a two-sample unpaired t-test using SPM12 (UCL, London, UK) in MATLAB software (MathWorks, Natick, MA, USA) setting a significance level threshold of 0.05 (uncorrected for multiple comparisons) and a minimum cluster size of 100 voxels.

Statistics

Data were analyzed using statistical software (Graphpad Prism 7, La Jolla, CA, USA). Regional differences between time points were analyzed by ANOVA followed by Dunnett's post hoc test with baseline animals as control group. Differences were considered statistically significant if $p < 0.05$. Data are shown as mean \pm standard deviation (SD).

Results

^{99m}Tc -HMPAO uptake normalization to the injected dose showed a decrease in the cerebellum during SE (-28%; $p = 0.042$) using the ROIs atlas analysis (Fig. 1A,B). During SE, this analysis method revealed no other significant differences. Twenty-four hours after SE, ^{99m}Tc -HMPAO SPECT showed a generalized

uptake reduction compared to baseline affecting mainly the dorsal hippocampus (-39%; $p = 0.008$), cortical regions (e.g. piriform cortex: -50%; $p < 0.001$), and cerebellum (-43%; $p < 0.001$). Brain perfusion in the chronic epileptic phase did not differ from baseline values

On the other hand, SPM analysis showed local alterations in ^{99m}Tc -HMPAO uptake of different extent at every studied time point (Fig. 1C). Parametric mapping showed an increased ^{99m}Tc -HMPAO uptake in localized cortical regions 15 minutes after the first pilocarpine injection, i.e. before the first seizure. Already during the first seizure, we found a significant decrease of ^{99m}Tc -HMPAO uptake in cortical sub-regions. This decrease in ^{99m}Tc -HMPAO was also present during the SE, mainly affecting cortical and cerebellar regions. SPM analysis confirmed the ROIs results, showing a generalized uptake reduction at 24 hours after SE. It also revealed decreased ^{99m}Tc -HMPAO uptake in cortical and hippocampal sub-regions in chronic epileptic rats.

Discussion

Here, we investigated brain perfusion during and after SE induced by lithium-pilocarpine in rats by brain imaging without the influence of anesthesia. After initial hyper-perfusion before SE onset, regional perfusion deficits during SE and acute epileptogenesis, as well as during chronic epilepsy became apparent.

A decrease in brain perfusion has previously been shown to correlate with later neuronal damage in adult animals [14]. Metabolic requirements during SE are increased due to higher glucose and oxygen demand [15]. We have previously shown an increased glucose consumption at 4 and 24 hours after SE in the pilocarpine rat model [5]. However, ^{99m}Tc -HMPAO SPECT imaging showed region-specific perfusion reduction during SE and whole-brain reduction at 24 h post SE despite an initial increase of cortical perfusion after pilocarpine injection. This divergence between metabolic requirements and perfusion during the SE may induce cell stress and lead to neuroinflammation and neuronal death already described in this animal model [6]. The initial increase of perfusion in cortical regions suggests involvement of these regions in the initiation of the SE by the systemic injection of pilocarpine. Previously, two MRI studies have also shown a decrease of brain perfusion in epilepsy-related areas during SE induced by pilocarpine in rats [16, 17]. However, an initial cortical activation directly after SE onset was observed in both MRI-based studies, while we found hypo-perfusion in cortical regions directly after the first convulsive seizure. Differently to these published studies [16, 17], anesthesia is not influencing our perfusion imaging as ^{99m}Tc -HMPAO uptake is taking place in awake animals. As the tracer gets trapped, animals can be later anesthetized for the scan without influencing uptake. Thus, differences in these studies may be due to alterations of cerebral blood flow and SE and the inhibition of convulsions due to the use of anesthesia [8].

Twenty-four hours after SE, we observed a generalized decrease of cerebral perfusion, mainly affecting cortical regions. Cortical regions have shown neuronal loss already hours after SE [18]. This early neuronal loss may be associated with the reduction of blood flow acutely after SE. In addition, we have

previously shown early reduction in neurotransmitter receptor density and amino acid metabolism 24–48 hours after SE [4, 5], which may be at least partially unchained by the hypo-perfusion-induced neuronal death as seen by ^{99m}Tc -HMPAO SPECT results obtained from the present study.

In addition, chronic epileptic animals also showed hypoperfusion localized in cortical and hippocampal regions. These areas have been described to be affected by neuronal loss and atrophy [19, 20] together with an enlargement of the ventricles [21] at this time point in the rat pilocarpine model. Since we did not have the option to perform individual MRI scans, we used a standard MRI template based on naive Sprague Dawley rats. Because of eventual atrophic changes induced by chronic epilepsy, hippocampus and cortical ROIs might include ventricle areas in chronic epileptic animals. This might explain a part of the reduction of perfusion as well as the decreases of glucose and amino acid metabolism previously described by our group [5].

SE induces brain regional hypoperfusion. Insufficient blood perfusion together with elevated energy requirements during SE may lead to neuronal damage and neuroinflammation, which are theorized to participate in the epileptogenic process. Counteracting perfusion deficiency during SE might therefore serve as a pharmacological target to ameliorate SE sequels.

Declarations

Ethics approval

All the experiments were conducted in accordance with European Communities Council Directive 2010/63/EU and were formally approved by the responsible local authority (Lower Saxony State Office for Consumer Protection and Food Safety).

Consent for publication

Not applicable.

Availability of data and materials

The datasets used and/or analysed during the current study are available from the corresponding author on reasonable request.

Competing interests

The authors declare that they have no competing interests.

Funding

This work was supported by the European Seventh's Framework Programme (FP7/2007-2013) under grant agreement n°602102 (EPITARGET). B. J. Wolf was supported by a scholarship of the

Studienstiftung des Deutschen Volkes. I. Jahreis and M. Brackhan were supported by a scholarship from the Konrad-Adenauer-Stiftung e.V.

Authors' contribution

Design of the study: PB, MBa, and JPB.

Data acquisition: PB, BJW, MBr, IJ, MBa, and LGG.

Analysis of experiments: PB, BJW, MBr, and IJ.

Writing of the manuscript draft: PB, BJW, MBa, and JPB.

Revision of the manuscript draft: All authors.

Acknowledgements

The authors thank A. Kanwischer, S. Eilert, P. Felsch, and S. Mehler for skillful assistance.

References

1. Walker MC. Pathophysiology of status epilepticus. *Neurosci Lett*. 2018;667:84-91. doi:10.1016/j.neulet.2016.12.044.
2. Hesdorffer DC, Logroscino G, Cascino G, Annegers JF, Hauser WA. Risk of unprovoked seizure after acute symptomatic seizure: effect of status epilepticus. *Ann Neurol*. 1998;44:908-12. doi:10.1002/ana.410440609.
3. Martín E, Pozo M. Animal models for the development of new neuropharmacological therapeutics in the status epilepticus. *Current neuropharmacology*. 2006;4:33-40. doi:10.2174/157015906775203002.
4. Bascunana P, Gendron T, Sander K, Jahreis I, Polyak A, Ross TL, et al. Ex vivo characterization of neuroinflammatory and neuroreceptor changes during epileptogenesis using candidate positron emission tomography biomarkers. *Epilepsia*. 2019. doi:10.1111/epi.16353.
5. Bascuñana P, Brackhan M, Leiter I, Keller H, Jahreis I, Ross TL, et al. Divergent metabolic substrate utilization in brain during epileptogenesis precedes chronic hypometabolism. *J Cereb Blood Flow Metab*. 2018;271678X18809886. doi:10.1177/0271678X18809886.
6. Brackhan M, Bascuñana P, Postema JM, Ross TL, Bengel FM, Bankstahl M, et al. Serial Quantitative TSPO-Targeted PET Reveals Peak Microglial Activation up to 2 Weeks After an Epileptogenic Brain Insult. *Journal of nuclear medicine : official publication, Society of Nuclear Medicine*. 2016;57:1302-8. doi:10.2967/jnumed.116.172494.
7. Meletti S, Monti G, Mirandola L, Vaudano AE, Giovannini G. Neuroimaging of status epilepticus. *Epilepsia*. 2018;59 Suppl 2:113-9. doi:10.1111/epi.14499.

8. Slupe AM, Kirsch JR. Effects of anesthesia on cerebral blood flow, metabolism, and neuroprotection. *J Cereb Blood Flow Metab.* 2018;38:2192-208. doi:10.1177/0271678X18789273.
9. Tikofsky RS, Trembath L, Voslar AM. Radiopharmaceuticals for Brain Imaging: The Technologist's Perspective. *Journal of Nuclear Medicine Technology.* 1993;21:57-60.
10. Lee DS, Lee SK, Lee MC. Functional neuroimaging in epilepsy: FDG PET and ictal SPECT. *J Korean Med Sci.* 2001;16:689-96. doi:10.3346/jkms.2001.16.6.689.
11. Andersen AR. 99mTc-D,L-hexamethylene-propylamine oxime (99mTc-HMPAO): basic kinetic studies of a tracer of cerebral blood flow. *Cerebrovasc Brain Metab Rev.* 1989;1:288-318.
12. Schiffer WK, Mirrione MM, Biegon A, Alexoff DL, Patel V, Dewey SL. Serial microPET measures of the metabolic reaction to a microdialysis probe implant. *Journal of Neuroscience Methods.* 2006;155:272-84. doi:10.1016/j.jneumeth.2006.01.027.
13. Schwarz AJ, Danckaert A, Reese T, Gozzi A, Paxinos G, Watson C, et al. A stereotaxic MRI template set for the rat brain with tissue class distribution maps and co-registered anatomical atlas: Application to pharmacological MRI. *NeuroImage;* 2006. p. 538-50.
14. Pereira de Vasconcelos A, Ferrandon A, Nehlig A. Local cerebral blood flow during lithium-pilocarpine seizures in the developing and adult rat: role of coupling between blood flow and metabolism in the genesis of neuronal damage. *J Cereb Blood Flow Metab.* 2002;22:196-205. doi:10.1097/00004647-200202000-00007.
15. Wasterlain CG, Fujikawa DG, Penix L, Sankar R. Pathophysiological mechanisms of brain damage from status epilepticus. *Epilepsia.* 1993;34 Suppl 1:S37-53. doi:10.1111/j.1528-1157.1993.tb05905.x.
16. Choy M, Wells JA, Thomas DL, Gadian DG, Scott RC, Lythgoe MF. Cerebral blood flow changes during pilocarpine-induced status epilepticus activity in the rat hippocampus. *Exp Neurol.* 2010;225:196-201. doi:10.1016/j.expneurol.2010.06.015.
17. Engelhorn T, Doerfler A, Weise J, Baehr M, Forsting M, Hufnagel A. Cerebral perfusion alterations during the acute phase of experimental generalized status epilepticus: prediction of survival by using perfusion-weighted MR imaging and histopathology. *AJNR Am J Neuroradiol.* 2005;26:1563-70.
18. Fabene PF, Merigo F, Galie M, Benati D, Bernardi P, Farace P, et al. Pilocarpine-induced status epilepticus in rats involves ischemic and excitotoxic mechanisms. *PLoS One.* 2007;2:e1105. doi:10.1371/journal.pone.0001105.
19. Peredery O, Persinger MA, Parker G, Mastrosov L. Temporal changes in neuronal dropout following inductions of lithium/pilocarpine seizures in the rat. *Brain Res.* 2000;881:9-17.
20. Bankstahl M, Bankstahl JP, Loscher W. Inter-individual variation in the anticonvulsant effect of phenobarbital in the pilocarpine rat model of temporal lobe epilepsy. *Exp Neurol.* 2012;234:70-84. doi:10.1016/j.expneurol.2011.12.014.
21. Niessen HG, Angenstein F, Vielhaber S, Frisch C, Kudin A, Elger CE, et al. Volumetric magnetic resonance imaging of functionally relevant structural alterations in chronic epilepsy after pilocarpine-induced status epilepticus in rats. *Epilepsia.* 2005;46:1021-6. doi:10.1111/j.1528-1167.2005.60704.x.

Figures

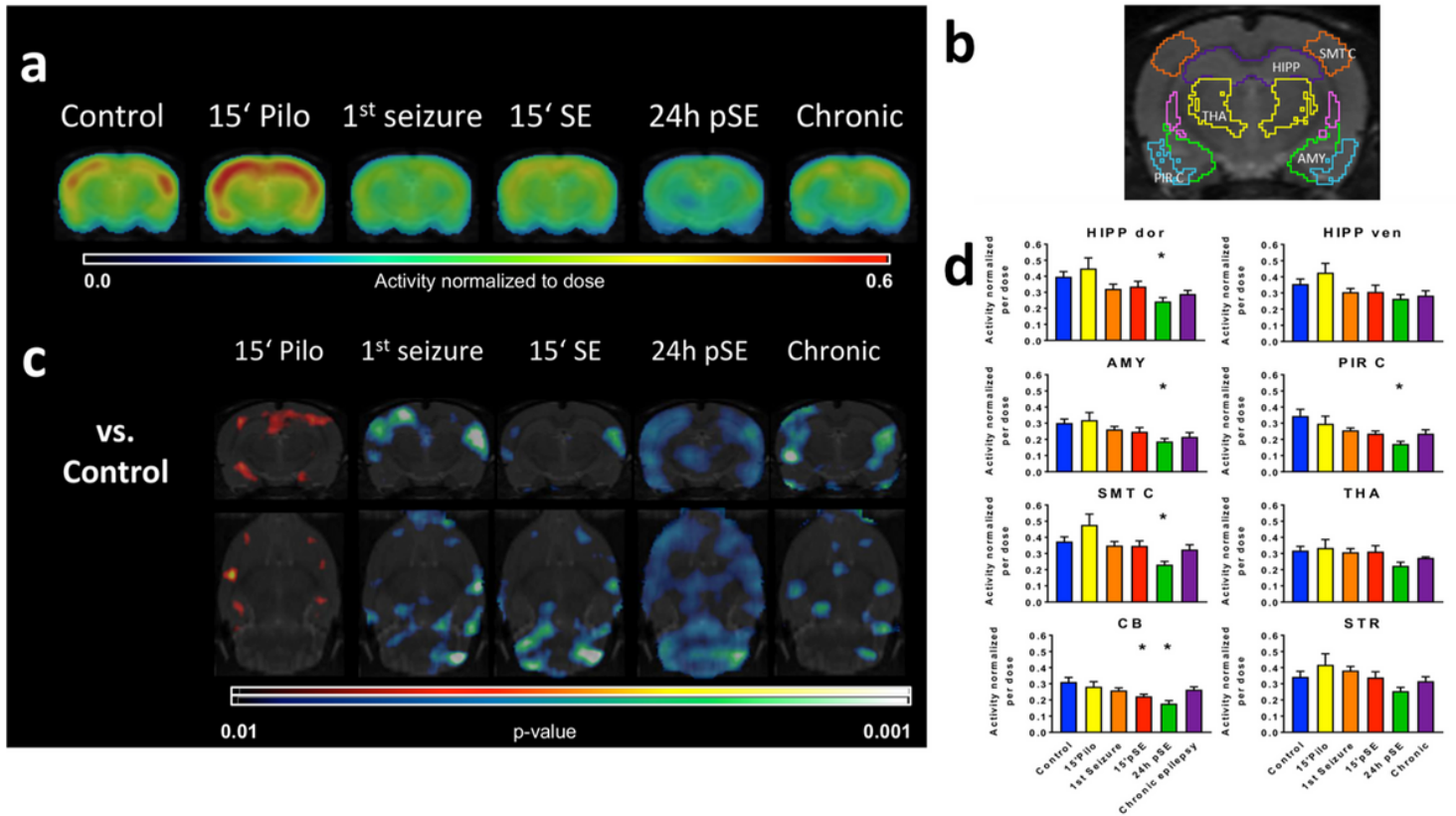


Figure 1

99mTc-HMPAO uptake normalized to the injected dose. (A) Coronal views from the average brain 99mTc-HMPAO uptake images fused to an MRI template for each experimental group. (B) Bar graph showing quantification of 99mTc-HMPAO uptake at the different time points in dorsal (HIPP dor) and ventral hippocampus (HIPP ven), amygdala (AMY), piriform cortex (PIR C), somatosensory cortex (SMT C), thalamus (THA), cerebellum (CB) and striatum (STR). Data are shown as mean±SD. Statistical analysis was performed by ANOVA and Dunnett's post hoc test. Asterisks indicate significant differences to the baseline group ($p < 0.05$). (C) SPM t-maps (in coronal and transversal views) showing significantly higher (hot scale) and lower (cold scale) uptake voxels at each time point compared to the baseline group ($p < 0.05$; minimum cluster size: 100 voxels).